



## Short communication

## All solid-state battery with sulfur electrode and thio-LISICON electrolyte

Takeshi Kobayashi<sup>a</sup>, Yuki Imade<sup>a</sup>, Daisuke Shishihara<sup>a</sup>, Kenji Homma<sup>a</sup>, Miki Nagao<sup>a</sup>, Ryota Watanabe<sup>b</sup>, Toshiyuki Yokoi<sup>b</sup>, Atsuo Yamada<sup>a</sup>, Ryoji Kanno<sup>a,\*</sup>, Takashi Tatsumi<sup>b</sup>

<sup>a</sup> Department of Electronic Chemistry, Interdisciplinary Graduate School of Science and Engineering, Tokyo Institute of Technology, 4259 Nagatsuta, Midori-ku, Yokohama 226-8502, Japan

<sup>b</sup> Chemical Resources Laboratory, Tokyo Institute of Technology, 4259 Nagatsuta, Midori-ku, Yokohama 226-8503, Japan

## ARTICLE INFO

## Article history:

Received 5 December 2007

Received in revised form 31 January 2008

Accepted 8 March 2008

Available online 22 March 2008

## Keywords:

Thio-LISICON

All solid-state battery

Sulfur electrode

## ABSTRACT

A high-capacity type of all solid-state battery was developed using sulfur electrode and the thio-LISICON electrolyte. New nano-composite of sulfur and acetylene black (AB) with an average particle size of 1–10 nm was fabricated by gas-phase mixing and showed a reversible capacity of 900 mAh g<sup>-1</sup> at a current density of 0.013 mA cm<sup>-2</sup>.

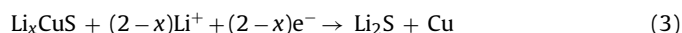
© 2008 Elsevier B.V. All rights reserved.

## 1. Introduction

Rechargeable lithium batteries have been developed for portable power storage applications. The practical capacities of the current system applicable for electric vehicles, for example, LiC<sub>6</sub>/LiCoO<sub>2</sub>, Li/LiMn<sub>2</sub>O<sub>4</sub>, Li/V<sub>6</sub>O<sub>13</sub> are normally in the range of 100–150 Wh kg<sup>-1</sup> (theoretical specific energies in the range of 425–890 Wh kg<sup>-1</sup>) [1], and further increases in battery specific energy have been expected. The battery capacity of the lithium ion system is mainly determined by the capacities of positive electrodes in the range of 150–200 mAh g<sup>-1</sup>, which are limited by the extent of lithium intercalation into transition metal oxides. Batteries based on the lithium/elemental sulfur redox couple might be a promising candidate for high-capacity battery. Sulfur has a theoretical specific capacity and specific energy of 1672 mAh g<sup>-1</sup> and 2600 Wh kg<sup>-1</sup>, respectively, with a reaction of S + 2Li<sup>+</sup> + 2e<sup>-</sup> ↔ Li<sub>2</sub>S [1]. However, high insulation of sulfur caused high electronic resistivity that makes only poor charge–discharge characteristics at low-temperature regions. The loss of active material in liquid electrolytes caused low active material utilization and poor rechargeability for the Li/S cells; during the charge–discharge process the sulfur transformed to polysulfides, which are soluble to the organic electrolyte. The incomplete reversibility of the reactions to lower-order sulfides (e.g. Li<sub>2</sub>S<sub>2</sub>, Li<sub>2</sub>S) was also a significant prob-

lem [2–6]. Sulfur has, therefore, not been sufficiently utilized in rechargeable lithium batteries with liquid electrolytes.

The Li/S batteries with solid polymer electrolytes have been examined in order to prevent polysulfides dissolving into liquid electrolytes [1,7,8]. However, total reversible discharge capacities of the cells were less than 30% of the theoretical capacity of sulfur even at higher operating temperatures around 100 °C. Low conductivity of polymer electrolytes might be one of the reasons for these results on the cells. On the other hand, all solid-state batteries using sulfur and ceramic solid electrolyte have been recently reported to have good cycle-performance [9]. Mechanically milled mixtures of elemental sulfur and a transition metal sulfide such as CuS act as a positive electrode with multiple reactions [10]:



and the cells showed high reversible capacities over 650 mAh g<sup>-1</sup> at room temperature. Good electronic conductivity of copper sulfide (CuS,  $\sigma = 67 \text{ S cm}^{-1}$ ; S,  $\sigma = 5 \times 10^{-30} \text{ S cm}^{-1}$  at 25 °C) makes the battery reaction reversible with high charge–discharge capacity [11,12].

We tried to use elemental sulfur as a positive electrode for all solid-state batteries. In the present study, all the solid-state lithium batteries with sulfur electrode and the thio-LISICON ceramic solid electrolyte [13] are examined to improve sulfur material utilization and thus the energy density of the batteries. Nano-composite of

\* Corresponding author.

E-mail address: [kanno@echem.titech.ac.jp](mailto:kanno@echem.titech.ac.jp) (R. Kanno).

sulfur and carbon was found to show high electrochemical capacity, and its reaction mechanism was investigated.

## 2. Experimental

The composite electrode of sulfur and acetylene black (AB) was fabricated through gas-phase mixing as follows. Sulfur (Kojundo Chemical Laboratory >99.99% purity) and AB (Denki Kagaku Kogyo K.K.) were weighed in the ratio of 50:50 (weight % (wt.%)), mixed in an argon-filled glove box, sealed in a quartz tube under vacuum atmosphere and heated at a fixed temperature of 300 °C. After heating, the tube was slowly cooled to room temperature. The composite electrode of sulfur and AB was also prepared by mechanical mixing. For the charge-and-discharge experiments of the solid-state cells, the cathode mixture of sulfur, AB, and thio-LISICON ( $\text{Li}_{3.25}\text{Ge}_{0.25}\text{P}_{0.75}\text{S}_4$ ) with a weight ratio of 25.0:25.0:50.0 was used. The cathode mixture was formed either by hand mixing or by Fritsch P-7 planetary ball milling apparatus. The test cell was composed of polyethylene terephthalate (PET) cylinder with an inner diameter of 10 mm. The solid electrolyte (thio-LISICON) of about 70 mg was pressed into a pellet. The cathode mixture of 5 mg was subsequently pressed onto one side of the electrolyte-pellet at 500 MPa. The anode was a combination of aluminum foil (0.1-mm thickness) and lithium foil of 0.1-mm thickness with a diameter of 10 mm. Its Li/Al ratio is about 38 mol% and its potential is 0.38 V vs. Li/Li<sup>+</sup>. The aluminum was attached to the solid electrolyte by a pressure of 500 MPa [14]. The preparation and fabrication of the cells was carried out in a dry argon-filled glove box ([H<sub>2</sub>O] below 0.1 ppm, Miwa MFG Co., Ltd.). The electrochemical properties were characterized by a multi-channel galvanostat (TOSCAT-3100). A cycling test was performed between 0.5 and 2.7 V at an applied current of 0.013–0.13 mA cm<sup>-2</sup> at 25 °C. The resistivity of the cells was examined at 1.5 V by an ac impedance method in an applied frequency range of 10 mHz and 1 MHz, and an applied ac voltage of 10 mV using a Solartron 1260 frequency response analyzer.

These electrodes were characterized by powder X-ray diffraction measurements using a Rigaku RU-200B with Cu K $\alpha$  radiation, and the weight ratio of sulfur and AB in the composite electrode was measured by CHNS analysis using a PerkinElmer 2400 and thermogravimetry (TG). TG measurements were conducted up to 600 °C from room temperature under nitrogen atmosphere. Morphologies of the composite electrodes fabricated by mechanical or gas/solid mixing were investigated by a field emission scanning electron microscope (FESEM) (Hitachi S-5200). The porosity considering open pores of the cathode composite was measured by Brunauer–Emmett–Teller (BET) measurement with nitrogen gas (Bellsorp. mini). The pore distribution of AB was refined by BJH method [15].

## 3. Results and discussion

Fig. 1 shows the X-ray diffraction patterns for the composite electrode of sulfur and AB prepared by a mechanical mixing with ball-milling apparatus, and gas/solid mixing, together with the pristine sulfur powder. The existence of sulfur was confirmed for the electrodes prepared by mechanical and gas/solid mixing. The diffraction peaks of sulfur in the electrodes prepared by the gas/solid mixing were broader than those in the mechanical composite, indicating that the gas/solid mixing made small sulfur particles. The particle sizes determined by the diffraction patterns were estimated to be about 110 and 500 nm for the solid/gas and mechanical mixing, respectively. A CHNS elemental analysis indicated that the composite electrodes with mechanical and gas/solid mixing have the sulfur/AB weight ratio of 50/50 and 27/73, respectively. These results are in agreement with the weight loss value of 30 wt.% determined from TG measurement to 300 °C for the composite electrode prepared by solid/gas mixing.

Fig. 2 shows charge–discharge curves of all the solid-state cells with the composite electrodes of sulfur and AB prepared by (a) mechanical mixing and (b) gas/solid mixing. The charge–discharge

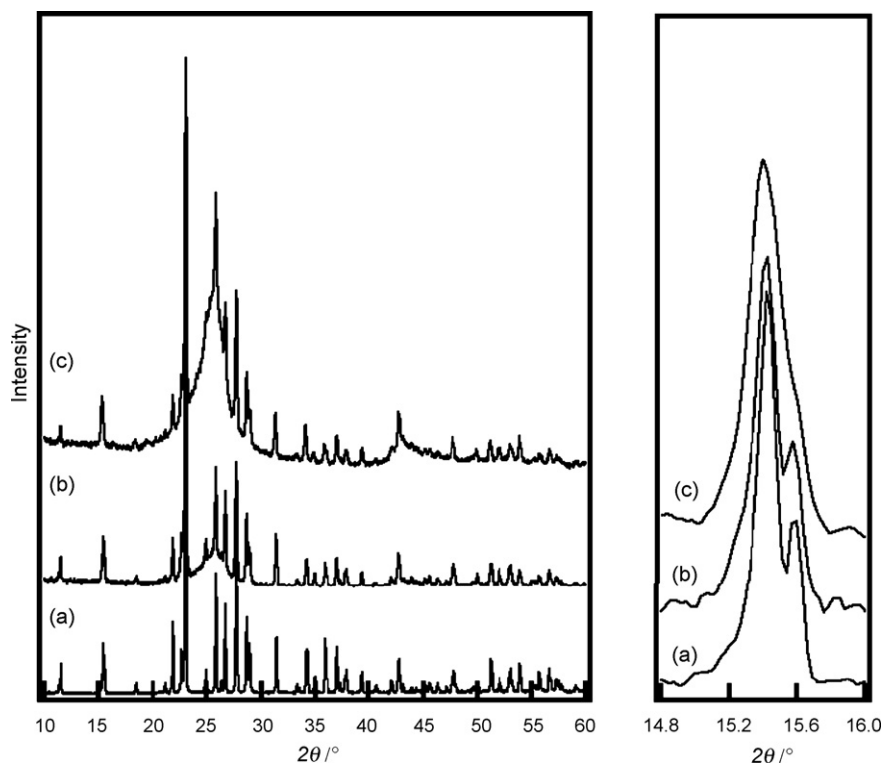
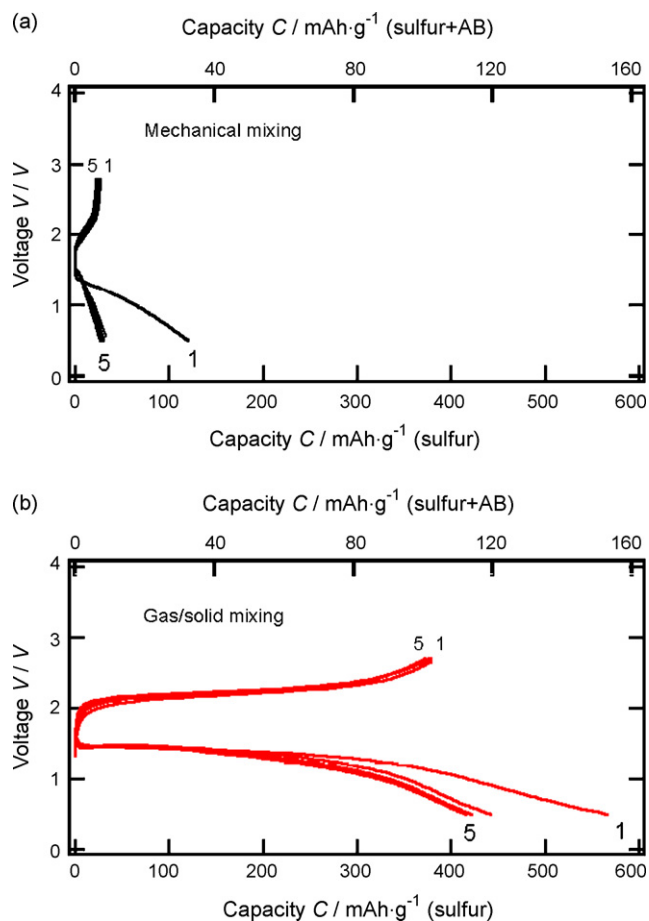
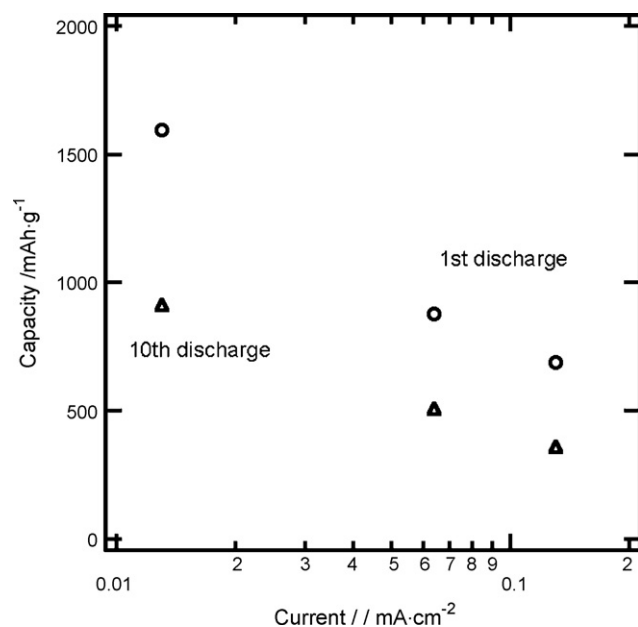


Fig. 1. X-ray diffraction patterns for the composite electrode prepared by (a) gas/solid mixing and (b) mechanical mixing. (c) X-ray diffraction patterns of the pristine sulfur.



**Fig. 2.** Charge–discharge curves of all solid-state batteries with AB/sulfur composite electrodes prepared by (a) mechanical mixing and (b) gas/solid mixing. The current density was  $0.13 \text{ mA cm}^{-2}$  with cut-off voltages of 0.5 and 2.7 V.



**Fig. 3.** Rate dependence of the charge–discharge capacity of the cell with AB/sulfur composite electrode prepared by gas/solid mixing. The rate dependence of the capacity was measured at the 1st cycle (circle) and the 10th cycle (triangle).

current was  $0.13 \text{ mA cm}^{-2}$ . These capacities were calculated based on the weight of sulfur. The cells of the electrodes with mechanical and gas/solid mixing have the first discharge capacities of 120 and  $590 \text{ mAh g}^{-1}$ , and the fifth discharge capacities of 30 and  $420 \text{ mAh g}^{-1}$ , respectively. The electrode preparation through sulfur gas process extremely improved the charge–discharge characteristics of all the solid-state cells using sulfur positive electrode.

Fig. 3 shows rate capability of all the solid-state cells using composite electrode prepared by gas/solid mixing. The discharge

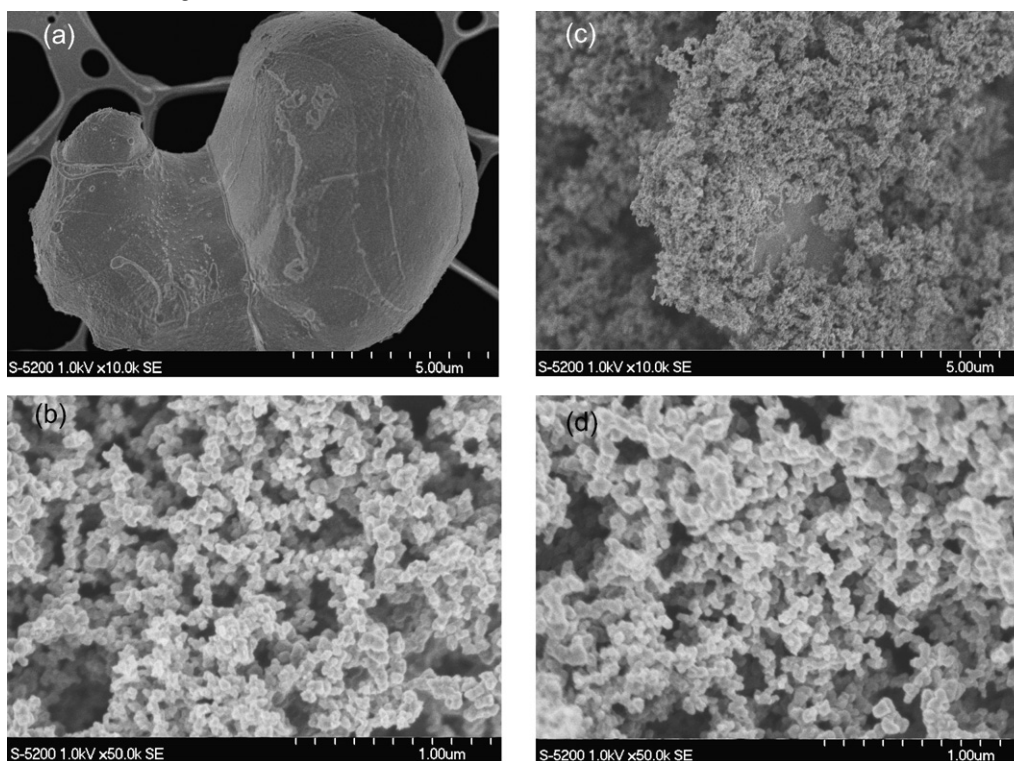


**Fig. 4.** Scanning electron microscope photographs of the composite electrode prepared by (a) sulfur, (b) acetylene black, (c) mechanical, and (d) gas/solid mixing.

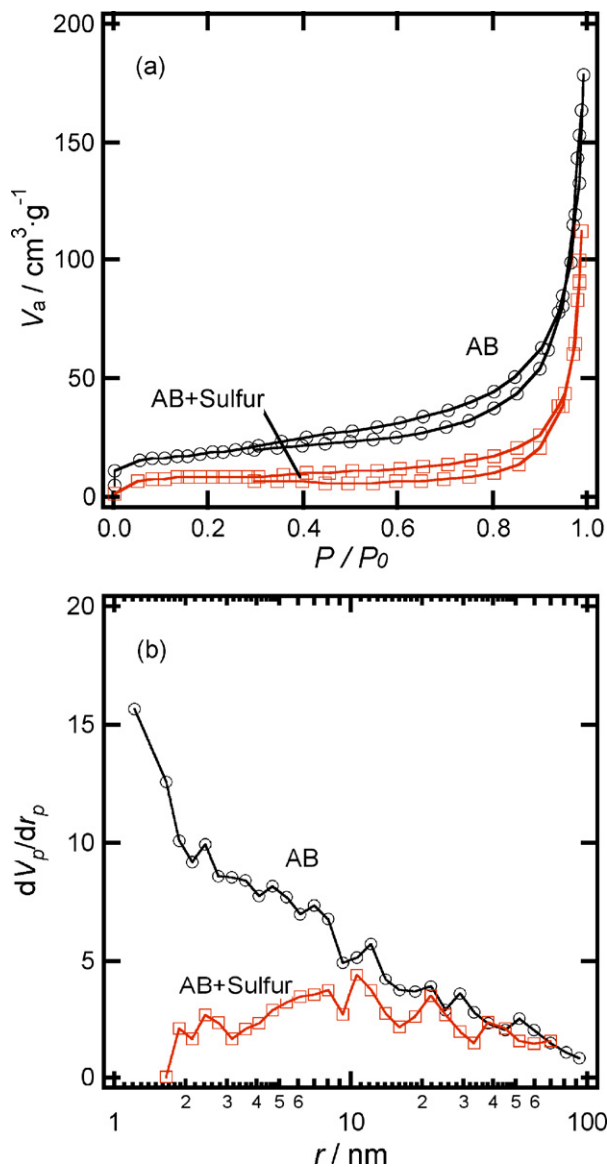


**Fig. 5.** (a)  $\text{N}_2$  adsorption–desorption isotherms (a) with corresponding pore size distributions (b) of the composite AB/sulfur electrodes prepared by mechanical and gas/solid mixing.

capabilities of the 1st and 10th cycle are plotted as a function of current densities in the range of  $0.013\text{--}0.13 \text{ mA cm}^{-2}$ . The large reversible capacity of  $900 \text{ mAh g}^{-1}$  was obtained with the current densities of  $0.013 \text{ mA cm}^{-2}$ . On the other hand, the capacities of high current densities of  $0.13 \text{ mA cm}^{-2}$  decreased to  $590 \text{ mAh g}^{-1}$ , implying that the polarization is still an important problem to be solved to attain high electrode utility at high current region.

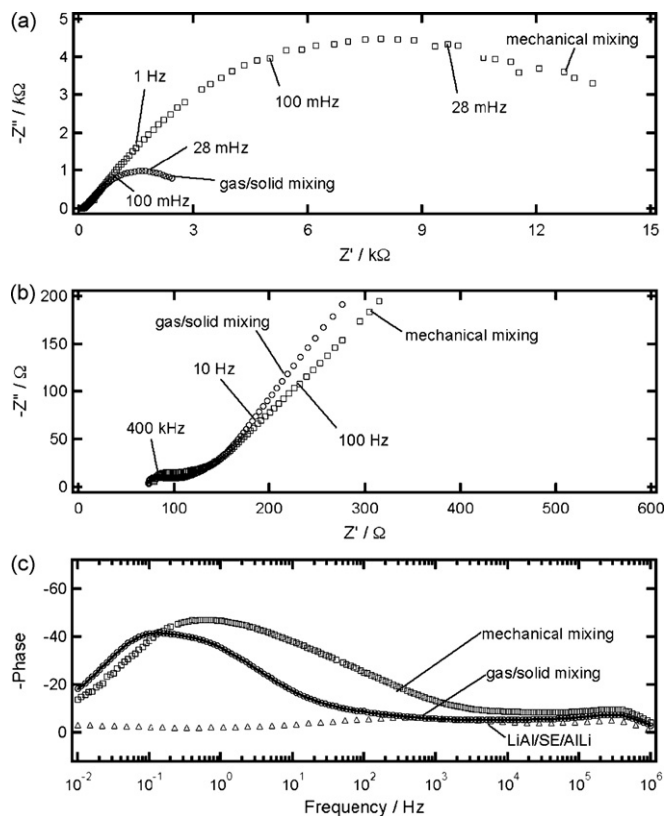
Fig. 4 shows the scanning electron microscope (SEM) photographs of pristine sulfur (a), AB (b), and the composites of sulfur and AB prepared by mechanical (c), and gas/solid (d) mixing. Large difference in the particle size was observed between the pristine sulfur ( $1\text{--}10 \mu\text{m}$ ) and AB ( $50\text{--}100 \text{ nm}$ ). After gas/solid mixing, the sulfur with large sizes of  $1\text{--}10 \mu\text{m}$  disappeared, while the particle size of the sulfur after the mechanical mixing remained unchanged ( $1\text{--}10 \mu\text{m}$ ), indicating that the deposition of sulfur from gas phase would lead to the successful formation of small particles.

Fig. 5(a) shows the  $\text{N}_2$  adsorption isotherms for the AB heated at  $300^\circ\text{C}$  and the composite electrodes prepared by solid/gas mixing, respectively. The BET surface areas of the AB and the composite

electrode were determined to be 66 and  $27 \text{ m}^2 \text{ g}^{-1}$ , respectively. The total volumes of the AB and the composite electrode were found to be  $0.27$  and  $0.18 \text{ cm}^3 \text{ g}^{-1}$ , respectively. Both the BET surface area and the total volume decreased with mixing. Fig. 5(b) shows the pore size distributions of AB heated at  $300^\circ\text{C}$  and the electrode mixed with sulfur at  $300^\circ\text{C}$ . The AB has pores with sizes ranging from 1 to 100 nm. After solid/gas mixing, the amount of pores decreased and the pore size decreased from 1–100 to 1–10 nm, suggesting that the pore of AB with the sizes of 1–10 nm was filled by sulfur. This is consistent with the results on the SEM observation that the solid/gas mixing caused homogeneous mixing with small sulfur particle sizes.

Fig. 6 shows ac impedance spectra (a and b) and impedance phase plots (c) for the composite electrodes with mechanical and gas/solid mixing. The Nyquist presentation of the spectra clearly reflects the multi-step nature of the overall lithium insertion and extraction process. Good separation of the relevant time constant was obtained, however, the semicircle corresponding to the bulk electrolyte was not observed in the high frequency region over 1 MHz. The impedance spectroscopy clearly demonstrated the reduction of electrode resistance by the solid/gas mixing. The two specific frequencies for the interfacial and charge transfer at the interface between Li–Al and solid electrolyte were also observed for both cells, which were 280 kHz and 410 Hz. These values have been already estimated from the symmetrical cell [14,16]. Therefore, each spectrum consisted of two semicircles in the high ( $>0.1 \text{ kHz}$ ), and low ( $<0.1 \text{ kHz}$ ) frequency regions which were assigned to the response of negative and positive electrodes, respectively [17,18].

The resistances of each component were obtained by least-square fittings of the ac impedance data using equivalent circuits of a combination of two  $R//\text{constant phase element (CPE)}$  and



**Fig. 6.** (a) ac impedance spectra for the composite AB/sulfur electrodes prepared by mechanical and gas/solid mixing, (b) impedance spectrum at high frequency region, and (c) impedance phase plots. These spectra were measured at 1.5 V.



the resistance of bulk electrolyte,  $R_b$  [19]. The resistivities of the anode and electrolyte are about  $70 \Omega$  [14,16], while the positive electrode showed much higher resistivities. The resistivities of the AB/sulfur electrode with solid/gas and mechanical mixing were 2.7 and  $14.8 \text{ k}\Omega$ , respectively. This indicates that the gas/solid mixing provided lower resistivities at the interface. Increase in the surface area and the contact between sulfur and AB reduced the interfacial resistance, which provided better electrochemical performance of all the solid-state cells.

#### 4. Conclusion

All solid-state cells with composite electrode with sulfur and AB were examined. The electrode preparation process using sulfur gas improved electrode utility during the charge–discharge process. Particle size of sulfur after gas/solid mixing was 1–10 nm; nano-size particles fabricated by the mixing process play an important role for the high charge–discharge capacities. The extremely high capacity obtained for the composite electrode was due to a close contact between sulfur and AB which acts as conducting matrix. The ac impedance spectroscopy indicated low resistivity for the composite electrode fabricated by gas/solid mixing. All the solid-state cells using sulfur electrode with composite electrode structure are promising candidate for lithium batteries for the next generation.

#### Acknowledgements

This work was partly supported by a Grant from The Ministry of Economy, Trade and Industry of Japan, and by a grant-in-aid

from The Ministry of Education, Culture, and Sports, Science and Technology of Japan.

#### References

- [1] D. Marmorstein, T.H. Yu, K.A. Striebel, F.R. McLarnon, J. Hou, E.J. Cairns, J. Power Sources 89 (2000) 219.
- [2] R.D. Rauh, K.M. Abraham, G.F. Pearson, S.K. Surprenant, S.B. Brummer, J. Electrochem. Soc. 126 (1979) 523.
- [3] H. Yamin, E. Peled, J. Power Sources 9 (1983) 281.
- [4] H. Yamin, A. Gorenshtein, J. Penciner, Y. Sternberg, E. Peled, J. Electrochem. Soc. 135 (1988) 1045.
- [5] G.G. Bikbaeva, A.A. Gavrilova, V.S. Kolosnitsyn, Russ. J. Electrochem. Soc. 29 (1993) 715.
- [6] J. Shim, K.A. Striebel, E.J. Cairns, J. Electrochem. Soc. 149 (2002) A1321.
- [7] B.H. Jeon, J.H. Yeon, K.M. Kim, I.J. Chung, J. Power Sources 109 (2002) 89.
- [8] X. Yu, J. Xie, J. Yang, K. Wang, J. Power Sources 132 (2004) 181.
- [9] N. Machida, K. Kobayashi, Y. Nishikawa, T. Shigematsu, Solid State Ionics 175 (2004) 247.
- [10] A. Hayashi, T. Ohtomo, F. Mizuno, K. Tadanaga, M. Tatsumisago, Electrochim. Acta 50 (2004) 893.
- [11] J.A. Dean (Ed.), Lange's Handbook of Chemistry, 3rd ed., McGraw-Hill, New York, 1985, pp. 3–5.
- [12] N.B. Hannay, Semiconductors, Reinhold, New York, 1959.
- [13] R. Kanno, M. Murayama, J. Electrochem. Soc. 148 (2001) 742.
- [14] R. Kanno, M. Murayama, T. Inada, T. Kobayashi, K. Sakamoto, N. Sonoyama, A. Yamada, S. Kondo, Electrochem. Solid-State Lett. 7 (2004) A455.
- [15] E.P. Barrett, L.G. Joyner, P.P. Halenda, J. Am. Chem. Soc. 73 (1951) 373.
- [16] T. Kobayashi, T. Inada, N. Sonoyama, A. Yamada, R. Kanno, in: Material Research Society Fall Meeting Proceedings, 2004, K11.1.
- [17] N. Ohta, K. Takada, L. Zhang, R. Ma, M. Osada, T. Sasaki, Adv. Mater. 18 (2006) 2226.
- [18] S. Seki, Y. Kobayashi, H. Miyashiro, Y. Mita, T. Iwahori, Chem. Mater. 17 (2005) 2041.
- [19] ZPLOT and ZVIEW for Windows, Scribner Associates Inc., North Carolina, USA, 1990–2007.